Eur Biophys J (2001) 30: 53–62
DOI 10.1007/s002490000107

ARTICLE

**Lisa H. Pope · Martyn C. Davies
Charles A. Laughton · Clive J. Roberts
Saul J.B. Tendler · Philip M. Williams**

Force-induced melting of a short DNA double helix

Received: 15 June 2000 / Revised version: 31 August 2000 / Accepted: 31 August 2000 / Published online: 18 November 2000

Abstract The dynamic behaviour of DNA is of fundamental importance to many cellular processes. One principal characteristic, central to transcription and replication, is the ability of the duplex to "melt". It has recently been shown that dynamic force spectroscopy provides information about the energetics of biomolecular dissociation. We have employed this technique to investigate the unbinding of single dodecanucleotide molecules. To separate the duplex to single-stranded DNA, forces ranging from 17 to 40 pN were required over a range of loading rates. Interpretation of the dependence of melting force on loading rate revealed that the energy barrier to rupture is between 9 and 13 kcal mol^{-1} in height and situated 0.58 nm from an intermediate structural state. Thermal melting studies show that, prior to dissociation, the oligonucleotide underwent a transition which required between 7 and 11 kcal mol^{-1} in energy. Through combined dynamic force spectroscopy and thermal melting studies we show the derivation of an energy landscape to dissociate a 12-mer duplex. Until very recently, this type of information was only accessible by computational analysis. Additionally, the force spectroscopy data allow an estimation of the kinetics of duplex formation and melting.

Key words Atomic force microscopy · DNA · Dynamic force spectroscopy · Melting · Stretching

L.H. Pope · M.C. Davies · C.J. Roberts · S.J.B. Tendler
P.M. Williams (✉)
Laboratory of Biophysics and Surface Analysis,
School of Pharmaceutical Sciences,
The University of Nottingham,
Nottingham NG7 2RD, UK
E-mail: phil.williams@nottingham.ac.uk
Tel.: +44-115-9515025; Fax: +44-115-9515110

C.A. Laughton
Cancer Research Laboratories,
School of Pharmaceutical Sciences,
The University of Nottingham,
Nottingham NG7 2RD, UK

Abbreviations *AFM:* atomic force microscopy · *DNA:* deoxyribonucleic acid · *SAM:* self-assembled monolayer · *XPS:* X-ray photoelectron spectroscopy

Introduction

Significant advances have been made in the manipulation of single molecules of deoxyribonucleic acid (DNA). In particular, stretching and force-induced melting of DNA has been achieved successfully through the techniques of optical tweezers, micro-pipette suction and the atomic force microscope (AFM) (Smith et al. 1992, 1996; Cluzel et al. 1996; Noy et al. 1997; Léger et al. 1999; MacKerrel and Lee 1999; Rief et al. 1999; Strunz et al. 1999). These studies reveal detailed information about both the mechanical properties of DNA and the forces required to separate duplex DNA into its constituent single strands. Whilst the response to mechanical stress has been investigated, little experimental correlation to thermodynamic and energetic descriptors has been made.

Pioneering work of Lee et al. (1994) demonstrated that forces required to separate strands of DNA could be measured using the AFM, and forces of 410 pN were required to separate double-stranded oligonucleotides of 12 base pairs [$d(ACTG)_3$ and $d(CAGT)_3$] in 0.1 M NaCl [the rupture force was reported at 830 pN and later corrected (MacKerrel and Lee 1999)]. Similar experiments were undertaken by Noy et al. (1997) using two complementary 14-mers with the sequence d(TCGGACAATGCAGA)·d(TCTGCATTGTCCGA), ensuring "all-or-none" type binding. Here, strand separation forces of 450 pN were recorded in 0.9 M NaCl. Recently, MacKerell and Lee (1999) repeated the first AFM experiments and measured rupture forces for the 12-mer of 130 pN, although this time in 0.01 M NaCl. Strunz et al. (1999) reported even smaller rupture forces for a 10-mer d(TAGCGTTGCC)·d(GGCAACGCTA) of between 22 and 42 pN (0.12 M NaCl), where the rupture force was dependent on the rate at which the strands were forced apart.

In addition to these studies of short oligonucleotides, the response of long double-helical strands of DNA to tensile stress has been investigated, initially by Bustamante and co-workers using optical tweezers (Smith et al. 1992). At forces of and above 10 pN the DNA was shown to behave elastically, the properties of which could be modelled by a worm-like chain. However, at around 70 pN the DNA yields abruptly and extends, reversibly, to approximately twice its natural length (the so-called B $\rightarrow$ S transition) (Cluzel et al. 1996; Smith et al. 1996; Rief et al. 1999). Recent AFM data have shown that, following this extension, random-sequence DNA can be induced to melt, identified by the strands adopting the mechanical properties of single strands, under forces of 150 pN (Rief et al. 1999).

It is interesting to note that the 460 pN force reported to unbind a 14-mer is much greater than that reputed to melt long random-sequence DNA (150 pN) (Rief et al. 1999). Furthermore, in the AFM 14-mer study an increased force was also reported for the B $\rightarrow$ S DNA transition, 120 pN, compared with 65–70 pN found by both optical tweezers and recent AFM measurements on DNA several thousand base pairs in length (Smith et al. 1996; Rief et al. 1999). Whilst the pathways for unbinding of short and long strands are undoubtedly different, it is counterintuitive that a short strand should be able to withstand higher stresses than one much longer.

Recent work into the study of the interactions of proteins and lipids has focused on the dynamic strength of adhesive bonds (Evans 1999; Merkel et al. 1999). Held together by an energy penalty, two interacting bodies will remain associated until thermal fluctuations overcome the energy potential. Thus, an interaction has a finite lifetime. The force required to break an interaction depends, therefore, on the timescale over which the force is applied, and will lie somewhere between zero (if the timescale is longer than the natural lifetime) and the maximum gradient of the energy potential. Between these two limits of time, the rupture force depends on the rate of force loading, study of which reveals details of the interaction potential (Evans 1999). This dynamic force spectroscopy has been used to study protein/ligand (Merkel et al. 1999), immunoglobulin/protein receptor (Simson et al. 1999) and oligonucleotide/oligonucleotide (Strunz et al. 1999) interactions.

It is the AFM results of Lee et al. and Noy et al. that were the inspiration for these studies, in which we attempt to understand the anomalies in rupture force through the application of force spectroscopy and further our knowledge of the behaviour of oligonucleotides under stress. We employed AFM to investigate the mechanical properties of a dodecamer and its force-induced melting over a range of loading rates. This technique of dynamic force spectroscopy allows the energetics of dissociation to be studied (Evans 1999; Merkel et al. 1999), by which the results can be compared to both thermodynamic and computational results. Using dynamic force spectroscopy, we profile the dissociation energy landscape as a dodecanucleotide is forced to melt into its constituent single strands. Combined with thermal melting studies, we are able to predict both barrier location and size. By analysing the interaction from an energetic perspective we are able to predict that the short oligonucleotide undergoes some degree of gross conformational change (a stretch) under force. We also estimate the base-pair dissociation energy and determine an association rate constant for the duplex. In comparison to studies of long DNA, it is expected that our short dodecanucleotide will provide important information about specific sequence-related thermodynamic characteristics.

Materials and methods

Surface functionalization

AFM probes and substrates were functionalized using the technique described by Noy et al. (1997). This involved the use of gold thiol chemistry to covalently attach single-stranded oligonucleotides in a well-characterized manner. Mixed self-assembled monolayers (SAMs) of oligonucleotides tethered to alkanethiols and alcohol thiols were generated by this procedure. Single-stranded oligonucleotides of sequence d(CGCAAAAAAGCG) were tethered to the gold substrate via hexadecanethiol and, similarly, gold-coated probes were functionalized with the complementary oligonucleotide d(CGCTTTTTTGCG). The alkane chains served to displace the DNA away from the surface and also to generate enough conformational freedom to promote recognition and binding with the complementary partner molecule in duplex formation. The mixed SAM of oligonucleotides with undecanol-thiol molecules was employed to space the oligonucleotides over the surface and promote single rather than multiple oligonucleotide-oligonucleotide interactions (1 in 200 dilution of surface functionality). The oligonucleotides were attached via their 5′ ends in order to study DNA stretching and melting rather than unzipping. The DNA sequence was chosen on the basis of an "all-or-none" type of binding to avoid collecting force-distance data from duplex DNA formed by partial overlap of the constituent single strands.

Template stripped gold substrates (Hegner et al. 1993) and gold-coated cantilevers were incubated overnight in a solution containing 1 μM hexadecanediol-5′-thiophosphate-oligonucleotides (solid-phase synthesis and FPLC purification by Oswel Research Products, University of Southampton, UK), 200 μM undecanol-thiol, 75% ethanol and 40 mM Tris buffer (pH 7). Following incubation the functionalized probes and surfaces were rinsed in deionized water to remove loosely bound material, stored in 20 mM Tris buffer (pH 7) and used on the same day for AFM experiments. All solutions were filtered prior to use.

Functionalization of control surfaces

For the study of non-complementary interactions, surface functionalization was carried out using the same procedure as for the complementary oligonucleotides. Interactions of d(CGCAAAAAAGCG) with d(CGCAAAAAAGCG) and of d(CGCTTTTTTGCG) with d(CGCTTTTTTGCG) were recorded. Undecanol SAMs were generated using the same procedure but without the 1 μM hexadecanediol-5′-thiophosphate-oligonucleotides. Oligonucleotide SAMs were generated using solutions containing 100 μM hexadecanediol-5′-thiophosphate-oligonucleotides and without the undecanol-thiol present.

X-ray photoelectron spectroscopy analysis of the functionalized surfaces

High resolution X-ray photoelectron spectroscopy (XPS) was used in order to confirm that there were no competitive binding effects

between the alcohol-thiol molecules and the oligonucleotide-thiol molecules in the generation of the mixed SAM (1:200 dilution of oligonucleotide functionality). Control surfaces of 100% oligonucleotide and 100% alcohol were used and all samples were prepared as described earlier. Prior to mounting within the XPS, the samples were rinsed extensively with HPLC grade ethanol. A VG Scientific Sigma Probe instrument with microfocus monochromatic Al K_α X-ray source was used for the analysis (VG Scientific, East Grinstead, West Sussex, UK). Survey scans were acquired from all samples, using a 400 μm monochromated X-ray spot, and high-resolution spectra collected in the regions of C 1s, N 1s, O 1s, P 2p, S 2p and Au 4f. Using an automated sample stage a number of analysis points were collected from the diluted oligonucleotide sample, each point being separated by 800 μm.

Force-displacement measurements

Cantilever deflection versus piezo displacement data were collected using an AFM constructed in the laboratory, controlled using commercial software (ThermoMicroscopes, Sunnyvale, Calif., USA). Single point force measurements were made using a 2 μm z-axis piezo. A number of different cantilevers and a range of approach/retract speeds were used to generate apparent loading rates between 285 and 23,226 pN s^{-1}. All experiments were undertaken in an aqueous environment of 20 mM Tris buffer (pH 7) and 10 mM $MgCl_2$. Datasets of typically 1000 force curves were collected for each loading rate. Cantilever spring constants were determined using the procedure described by Cleveland et al. (1993) and ranged from 0.044 to 0.079 N m^{-1}.

Oligonucleotide thermal melting studies: Gibbs free energy to dissociation

The UV absorbance of 1, 2, 3 and 5 μM solutions of the duplex oligonucleotide (solid-phase synthesis and FPLC purification by Oswel Research Products, University of Southampton, UK), in 20 mM Tris buffer (pH 7) and 10 mM $MgCl_2$, were measured using a Pharmacia Biotech Ultrospec 2000 UV/Visible Spectrophotometer at a wavelength of 260 nm. The temperature of the solution was ramped from 20 to 90 °C at a rate of 1 °C per minute and the melting temperatures (T_m) obtained from the absorbance profile. Thermodynamic parameters, ΔH and ΔS, were extracted from the melting curves using the method of Petersheim and Turner (1983).

Theory

Theoretical considerations

AFM melting studies of long DNA double strands indicate that whilst the B → S transition is highly cooperative and the transition force is independent of the loading rate, the melting transition shows pronounced rate dependence (Rief et al. 1999). For our 12-mer oligonucleotide we expect many dissociation trajectories, and whilst our force is applied normal to the surface, we do not assume that the DNA is stressed axially. For our system held under a weak force (spring constant $K \approx 0.05$ N m^{-1}), thermal fluctuations of the restraint are significant [$\sqrt{(k_B T/K)} = 0.3$ nm] (Balsera et al. 1997) and, therefore, stretch is not inevitable and the unbinding pathway is not restricted. Under these conditions, direct mechanical correlations between the response of the force transducer and the status and behaviour of the molecule cannot be made. Here, therefore, we consider only the rupture force (as the maximum force experienced by the AFM probe on retraction) and the rate of force loading. The system is assumed to remain in the thermally activated regime and we consider the force-induced melting dynamics as a non-equilibrium process using the classical Kramers approach (Park and Sung 1999).

Profiling energy landscapes

Interpretation of experimental loading rate rupture data provides a method by which regions of the unbinding energy landscape can be mapped. Energy landscapes may have complex profiles over which there may be many different routes of dissociation; however, a bond or interaction may simply be considered as confinement by a single energy barrier positioned along a specific pathway to dissociation. The application of an external force on an interaction, over a given amount of time, results in the tilting of the energy landscape, hence governing the location and size of this barrier (Evans and Ritchie 1997; Evans 1999; Williams et al. 2000). For the case where dissociation involves disruption of more than one type of interaction, multiple barriers will exist. For this situation, controlled tilting of the landscape, by varying the loading rate, allows individual barriers to be examined in turn. Relating theory to experiment, it is possible to estimate both the positions and sizes of barriers encountered within the landscape. Ideally, extensive exploration in the loading rate can be used to reveal a detailed map of prominent barriers and their energies. The range of loading rates required is large, covering many orders of magnitude, and the AFM suffers due to its limited dynamic range.

AFM measurements of dissociation forces are usually plotted as histograms; subsequently, the maximum in this distribution reveals the most probable force for dissociation, F^*. Of particular relevance to interpretation of this force, first postulated by Bell (1978), tilting of the energy landscape, and hence lowering the barrier to unbinding, leads to exponential amplification of the dissociation kinetics. For the case of forced rupture, such as in AFM experiments, this force can be related to loading rate, r_F, through the equation:

$$F^* = f_\beta\left(\ln(r_F) - \ln\left(r_F^0\right)\right) \quad (1)$$

where f_β ($= k_B T/x_\beta$) is the thermal force scale, $k_B T$ is the thermal energy, x_β is the displacement in the force direction, r_F is the experimental loading rate and r_F^0 is the natural loading rate of the system (Evans 1999).

Results

Investigating the specificity and nature of the oligonucleotide interactions

In order to assess the specificity and nature of the interaction between the complementary oligonucleotide

strands, a number of control experiments were carried out. These included interactions between non-complementary strands, interactions between the spacer alcohol molecules and interactions between SAMs generated from solely complementary oligonucleotides (no dilution of surface functionality). Typically, a number of different types of cantilever deflection versus piezo displacement curves were observed in the AFM experiments owing to various tip-sample interactions. These were categorized as either (1) no adhesion between tip and substrate, (2) specific adhesion, (3) non-specific adhesion or (4) multi-specific/non-specific adhesion (Fig. 1). It is hence evident from both this work and a previous study (Willemsen et al. 1999) that non-specific and specific interactions are easily distinguishable by their form. For each control experiment the force data were assessed to determine the number of different interaction types (Table 1). The results from these control experiments show that specific adhesion events of type (2) are only observed for the mixed SAMs of complementary oligonucleotides. Since these specific interactions were typically observed at a rate of one per five force curves recorded, it is most probable that they represent single rather than multiple hybridization events. The specificity of interaction type (2) could further be confirmed since flooding the buffer system with excess of one of the single-stranded oligonucleotides eliminated this type of interaction, confirming that the recorded data were indeed representative of duplex melting. Using this method of force curve discrimination, data were selected such that only interactions between single pairs of complementary oligonucleotides were considered. All of the data presented from this point are solely representative of type (2), identified as specific single-molecule interactions between the complementary oligonucleotide strands. A polynomial fit to the force versus piezo displacement data allowed measurements of both the cantilever restoring force and the gradient of the curve at the point of DNA rupture, indicative of the true loading rate.

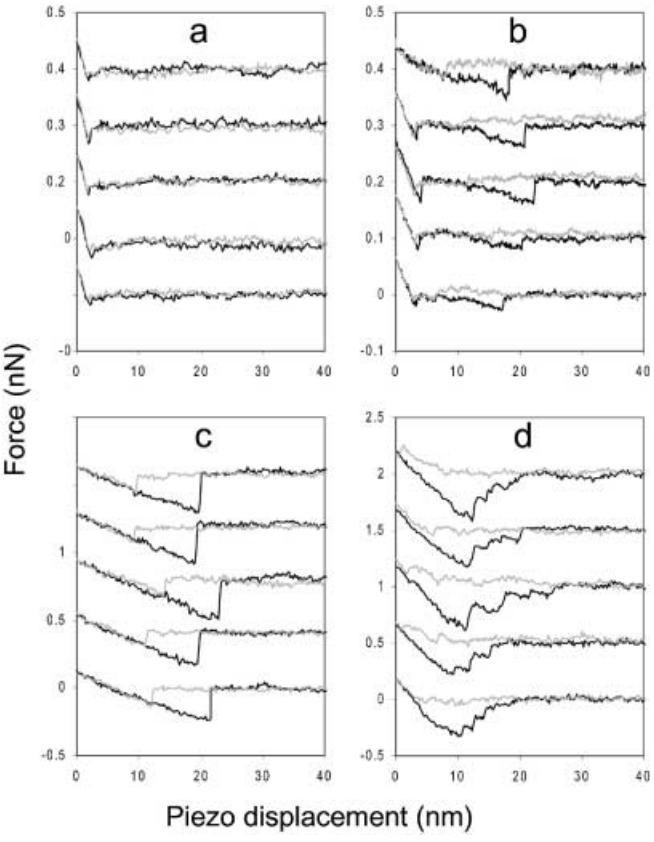

Fig. 1a–d A selection of the four different types of force versus piezo displacement curves collected for interactions between complementary oligonucleotides and various control surfaces. The retract curve is shown in *black* and hystereses between the approach and retract curves represent interaction forces between the probe and surface. These curves are of: **a** no adhesion, observed for all types of probe-substrate systems; **b** specific adhesion, identified by a non-linear force-displacement relationship, observed only for single-molecule interactions between complementary oligonucleotides, i.e. surfaces in which surface functionality of the single-stranded oligonucleotides were diluted 200-fold with undecanol-thiol spacer molecules; **c** non-specific adhesion, observed for all types of system and characterized by a sharp linear pull-off; **d** multi-specific adhesion, where multi attachments of the probe to the substrate can clearly be identified by discrete vertical steps as the probe breaks free of a number of different interactions/attachments in turn. This type of interaction was only observed where there was no dilution in surface density of the oligonucleotides

Surface characterization using XPS

In order to check that there were no competitive binding effects between the oligonucleotide-thiol molecules and the alcohol-thiol molecules, high-resolution XPS was

Table 1 Assessment of the specificity of tip-sample interactions in the identification of single-molecule oligonucleotide unbinding events[a]

	No adhesion	Specific	Non-specific	Multi-specific
Undecanol SAMs	45.9	0	54.1	0
Non-complementary	39.2	0	60.8	0
100% complementary	10.7	0	80.6	8.7
1:200 dilution complementary	41.3	21.4	37.3	0

[a] It is evident from these results that interactions between all of the different tip-substrate surface chemistries show some degree of no adhesion and non-specific adhesion. Multi-specific adhesion is only observed for interactions between surfaces of complementary oligonucleotides where there is no dilution of functionality. Specific single-molecule interactions are solely observed between surfaces of complementary oligonucleotides where surface functionality is reduced by 200-fold with alcohol spacer molecules

employed. Control surfaces of a 100% oligonucleotide SAM and 100% alcohol SAM were used alongside the 1:200 diluted oligonucleotide surface and particular attention was focused on the N, P and C contents of the samples (N and P being a specific finger print for the presence of DNA). The results from these studies showed that there was very little N present and no P present for the alcohol SAM [we believe that the small N content (0.38%) is due to contamination of the surface from either the Tris buffer or the mica surface prior to template stripping]. Comparing the observed and theoretical N/C and P/C ratios for the 100% oligonucleotide SAM and the 1:200 diluted oligonucleotide SAM revealed very close agreement, confirming a ~200-fold reduction in the amount of DNA present on the diluted surface. One notable aspect of the functionalized surfaces was that hydrocarbon contamination resulted in a C content approximately three times that theoretically calculated.

The force-loading rate relationship investigated through dynamic force spectroscopy

From the data collected for our dodecamer (measurements from specific single-molecule interactions), a histogram of rupture forces was plotted for each apparent loading rate, taken as the product of the cantilever stiffness (K_C) and piezo retract speed (V_R). A selection of these force distributions is illustrated in Fig. 2. Gaussian fits to each distribution were used to determine the most probable rupture force, F^*, and the standard deviation. The errors in force were calculated as the error in the fit of the Gaussian given by $2\sigma/\sqrt{N}$ (Strunz et al. 1999). An increase in F^* from 17 to 40 pN and a broadening in the range of forces was observed for apparent loading rates increasing from 285 to 23,226 pN s^{-1}. However, the rate at which the duplex was loaded cannot be assumed to equal the product $K_C V_R$ since the hexadecane linkers and gold substrates also comply and deform under force. The rate of loading for each rupture event was determined from the gradient of the force versus piezo displacement curve at strand separation multiplied by the cantilever retract velocity. This gave a distribution of forces over true loading rates from 100 to 2900 pN s^{-1}. The limited spread in loading rate achievable using AFM is evident. These data were sorted into increasing loading rate, forming 16 groups where Gaussian fits were obtained on the distributions of force within each. The change of force for each magnitude increase in loading rate (f_β) of 10 pN indicated a barrier 0.42 nm wide. As discussed previously, however, this assessment of loading rate is problematic since mechanical properties cannot be extracted directly from the force extension curve.

In order to assess the effect of the hexadecane linker on the rate at which the DNA was loaded, a comparison between apparent and true loading rate was made (Evans and Ritchie 1999). As described earlier, the stiffness of the cantilever/linker system (K_S) was measured from the gradient of the force data at the point of rupture. The stiffness of the "linker" (K_L) (which includes the effects of both the alkane linkers and the gold substrates) was determined approximately through a linear spring model by $K_L=(K_C K_S)/(K_C-K_S)$ and found to have a spring constant of 0.010 N m^{-1}, although the data

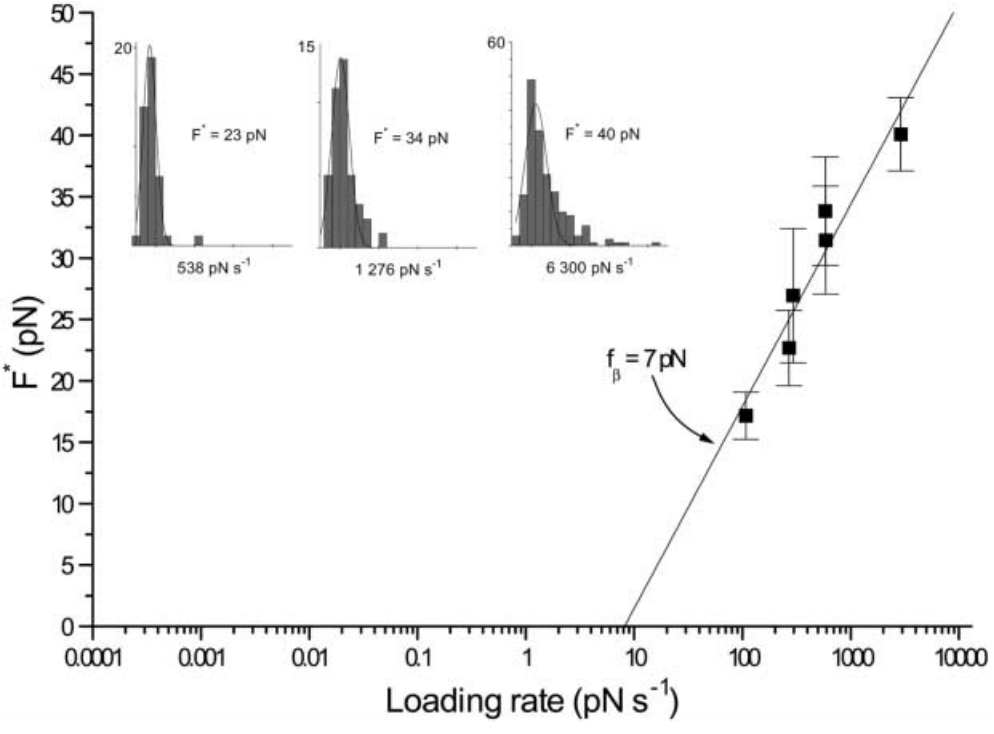

Fig. 2 Dynamic force spectroscopy of the 12 base pair oligonucleotide, over corrected loading rates from 100 to 2900 pN s^{-1}, reveals rupture forces with a logarithmic dependence on the loading rate. The force scale of 7 pN corresponds to a barrier displacement of 0.58 nm. *Inset*: rupture forces are determined from histograms taken from several hundred measurements at each loading rate. At an apparent loading rate of 538 pN s^{-1} (taken as the product of cantilever stiffness and retract speed) a peak in the force distribution is seen at 23 pN. As the apparent loading rate is increased to 6300 pN s^{-1}, both an increase in the peak position and the distribution width is seen

exhibited a large scatter (0.007 N m^{-1}). This value represents the entropic stiffness of the chains attaching the DNA to the tip and substrate, and neglects any loading-rate dependence. The unit modulus is of a similar value to that found for a 30 nm poly(ethylene glycol) linker used by Struntz et al. (1999).

From the oligonucleotide force spectroscopy data, a plot of F^* versus a corrected loading rate (taken as $K_S V_R$ where $1/K_S = 1/K_C + 1/0.010$) was made (Fig. 2). The linear dependence of F^* on the logarithm of the loading rate is in agreement with the theoretical description of forced bond rupture (Eq. 1) and indicates that the duplex melting is forced within the thermally active regime. This is expected for the experimental timescale involved and justifies our Kramers consideration. From the gradient of the slope ($f_\beta = k_B T/x_\beta = 7$ pN, s.d. = 0.99 pN) it can be determined that the energy barrier to melt the short double helix is situated (x_β) 0.58 ± 0.07 nm away from a stable structural state.

The displacement of the barrier of a few angstroms from a stable state suggests that either the molecule does not stretch in the experiment, or that a transition to a distal energy minimum is induced at forces below 17 pN. To determine whether a conformational change of significant energy penalty occurs under force we compared the size of the barrier predicted from the force spectroscopy to that measured in thermal melting studies.

Energetic consideration

The height of the barrier to rupture, E_r, can be determined from the force data since (Evans 1999):

$$E_r = k_B T\left(\ln\left(f_\beta\right) - \ln left(r_F^0\right) - \ln(t_D)\right) \quad (2)$$

However, Eq. 2 requires knowledge of a natural timescale, t_D, which is the reciprocal of the attempt frequency over the energy barrier. As shown by Kramers, in experiments of forced dissociation the molecular system obeys the same over-damped dynamics as condensed liquids and this attempt frequency is several orders lower than the $k_B T/h$ expressed with the Eryring equation used to explain the behaviour of gases. For streptavidin/biotin, for instance, the attempt frequency, $1/t_D$, is of the order of 1 ns^{-1}. Evans showed that the time constant is related to two length scales, l_c and l_{ts}, and a viscous damping term, γ, as $t_D = l_c l_{ts}(\gamma/k_B T)$. The length scales are derived from the curvature of the energy landscape at the bound and transition states, respectively. For our DNA we estimate $l_c l_{ts}$ to lie between 0.01 and 1 nm^2. For the streptavidin/biotin system, molecular dynamics (MD) studies indicated a damping term, γ, of 2×10^{-8} pN s nm^{-1} (Grubmüller et al. 1996), notably equivalent to the Stokes drag on a similar sized sphere in liquid (Evans 1999). Whilst similar MD simulations for DNA as a function of velocity have not been performed, the forces of 830 pN calculated by Konrad and Bolonick (1996) indicate that this damping is less than 1×10^{-7} pN s nm^{-1}, although total simulation times were not specified. Stokes drag on an oligonucleotide-sized sphere would be of the order of 5×10^{-8} pN s nm^{-1}. Using these values of $l_c l_{ts}$ and γ we can assume that the pre-factor, t_D, varies between 1 and 100 ns. Using both fits to the data (Fig. 2 and a plot of each individual F versus true loading rate) the value f_β/r_F^0 (thermal lifetime) is in the region of 1 s. The uncertainty in t_D gives rise to a considerable range in the possible height for the barrier E_r from 9 to 13 kcal mol^{-1}.

Estimation of the total free energy change on dissociation was possible through thermal melting studies of the 12-mer oligonucleotide under the buffer conditions of the force spectroscopy (10 mM $MgCl_2$). Thermodynamic parameters, ΔH and ΔS, were extracted from the melting curves by solving (Petersheim and Turner 1983):

$$\alpha/2(1-\alpha)^2 c_T = \exp(-(\Delta)H - T\Delta S)/k_B T \quad (3)$$

where α is the fraction of double stranded DNA and c_T is the total strand concentration. This procedure utilized Mathematica (Wolfram Research) and a combination of Newton-Raphson (Microsoft Excel) and downhill simplex minimizations (Press et al. 1992). These studies revealed a ΔH of 107.6 kcal mol^{-1} (s.d. = 4.2, $n = 12$) and a ΔS of 300.1 cal mol^{-1} K^{-1} (s.d. = 12.8, $n = 12$) (1 kcal mol^{-1} = 4.18 kJ mol^{-1} = 1.69 $k_B T$). As expected, the melting temperature was dependent on oligonucleotide concentration and increased from 55 to 60 °C as the concentration increased from 1 to 5 μM. Nearest neighbour predictions of free energy, in 1 M NaCl, are $\Delta H = 103$ kcal mol^{-1} and $\Delta S = 255$ cal mol^{-1} K^{-1} as described by Breslauer et al. (1986), and $\Delta H = 99$ kcal mol^{-1} and $\Delta S = 258$ cal mol^{-1} K^{-1} as described by Sugimoto et al. (1996). Extrapolation of these predicted ΔG_{37} from 1 M to 100 mM NaCl reveals a free energy of 13.5 kcal mol^{-1} (Nakano et al. 1999), which is in good agreement with the ΔG_{37} from our T_m measurements of 14.5 kcal mol^{-1}. At 20 °C, we calculate a free energy barrier ΔG in the 10 mM magnesium salt of 19.6 kcal mol^{-1} (s.d. = 0.48, $n = 12$).

Whilst the reaction coordinate for thermal and forced-induced melting may differ due to confinement of the latter by force, it is reasonable to expect that thermal melting requires a change in free energy no greater than that for force. Since the free energy from the thermal melting studies is significantly larger (20 kcal mol^{-1}) than the magnitude of the barrier predicted by dynamic force spectroscopy (13 kcal mol^{-1}), there must exist a structural change requiring a cost in energy of at least 7 kcal mol^{-1} that is not evident in the force data. Since force spectroscopy at the loading rates employed here predicts only one barrier, this conformational change occurs at forces below 17 pN and over a distance of at least 2.7 nm (since 1 kcal $mol^{-1} \approx 7$ pN nm). To probe this region of the energy landscape would require rates of loading many orders of magnitude lower than those accessible to AFM. Since the thermal force scale over a barrier 2.7 nm away from the bound state would be close

to 1.5 pN, measurement could be attempted only using very weak force transducers, such as by the biomembrane force probe (Evans et al. 1995).

From the combination of thermal and force melting studies we can predict two forms of the energy landscape traversed under force. There is a region 2.7 nm or longer over which a structural change occurs involving an increase in energy between 7 and 11 kcal mol^{-1} (as $\Delta G - E_r$). There is also a sharp barrier between 9 and 13 kcal mol^{-1} in height. This barrier could occur before or after the structural transition. Whilst we cannot reliably take measurement of extension from the force displacement data, it is possible to apply molecular modelling to indicate which form of the potential is correct.

Simulation of the force experiment directly through molecular mechanics is not possible since the timescale available for simulation is several orders smaller than that of the experiment and, at 1 ns, is less than the natural attempt time t_D. Thus dissociation in these simulations is not thermally activated and forces measured reflect friction and energy dissipation. However, potential of mean force calculations do allow the form of the energy landscape, for a particular trajectory, to be derived. In adiabatic mapping studies, Lebrun and Lavery (1998) showed that the energy of a 14-mer increases steadily as the duplex is stretched over 5 nm and then rises rapidly until rupture after a further 1 nm. Similarly, using molecular dynamics, both Konrad and Bolonick (1996) and MacKerrel and Lee (1999) showed a gradual increase in energy for a 12-mer over a 4 nm stretch followed by a sharp increase before rupture. These studies indicate that the energy landscape profiled by our force spectroscopy is one of a gradual increase over at least 2.7 nm followed by a sharp, sub-nanometre width barrier (Fig. 3a). However, the case of the sharp barrier preceding the transition cannot be discounted fully.

Under forces below 17 pN, the energy landscape is tilted sufficiently so that a new energy well, after the transition at 2.7 nm, is produced (Fig. 3b). Force spectroscopy, using the rates available by AFM, probe the barrier adjacent to this new minimum. Features along the stretch transition may not be visible to force spectroscopy, particularly if the landscape is concave in this region and barrierless. Experiments over a range of loading rates several orders lower than the 100 pN s^{-1} used here should reveal a second region of force scale, with a slope near 1 pN on the log scale.

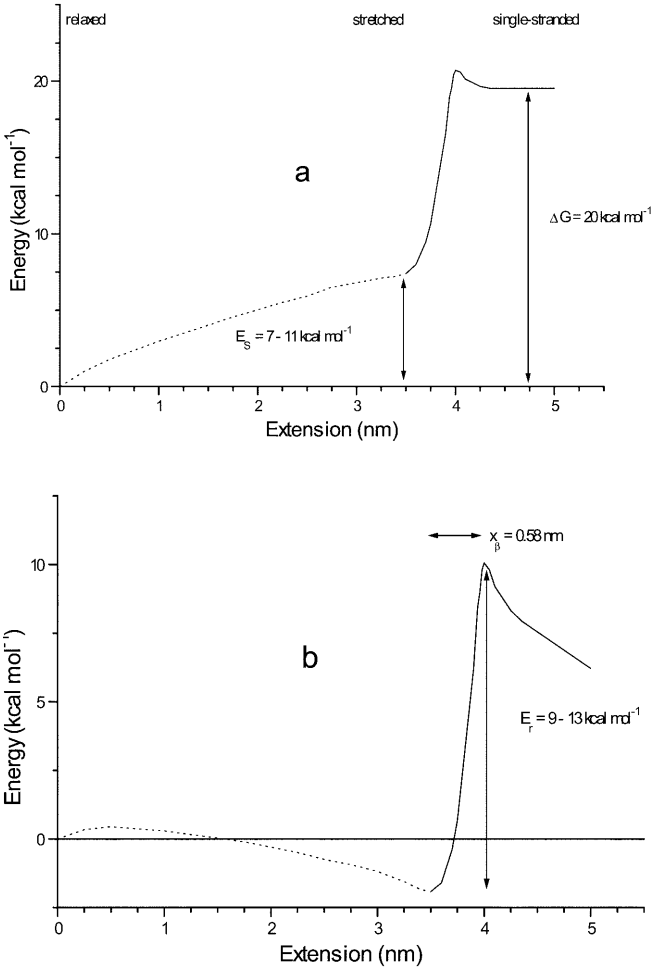

Fig. 3a, b Combined dynamic force spectroscopy and thermal melting studies permits the prediction of the energy landscape to stretch and rupture for the 12 base pair oligonucleotide. **a** The energy to stretch is between 7 and 11 kcal mol^{-1}, at forces below 17 pN. After stretch, a sharp barrier to rupture of between 9 and 13 kcal mol^{-1} in height is encountered. **b** Under forces greater than 17 pN the stretch region of the energy curve is suppressed, leaving a barrier to dissociation 0.58 nm wide. Under loading rates employed here by the force microscope, no contribution to the rupture forces from the energy landscape during stretch is seen

Oligonucleotide off- and on-rate calculations

The logarithmic intercept to the force plot with loading rate (Fig. 2) permits an estimation of the thermal off-rate by r_F^0/f_β, here determined between 0.2 and 1.7 s^{-1}. This compares with values derived from thermal melting studies of oligo(A)·oligo(U) duplexes, at 100 s^{-1} (Pörschke 1977), and force spectroscopy data of 0.001 s^{-1} from GC-rich oligonucleotides (Strunz et al. 1999). Interestingly, this measurement taken from the intercept of the log plot at zero force is not affected by the value of spring constant used (although the force scale, f_β, is) and can be derived from displacements of the force transducer alone.

A theoretical consideration of melting of oligonucleotides, undertaken first by Craig et al. (1971) and later supported by Anshelevich et al. (1984), suggests that the dissociation rate, v, for small base pair number, N, is related to the on-rate of base pair association, and approximated by:

$$v \approx 2k_f N / s^N \tag{4}$$

where s is the stability constant of a base pair interaction, as $s = k_f/k_b \approx exp(\delta G_{bp}/k_B T)$, and k_f and k_b are the on- and off-rates for a base pair interaction of ΔG_{bp}

in free energy. This dependence on the on-rate is known since duplex formation progresses from a critical intermediate, a region of several base pairs that can rapidly dissociate more quickly than it can react to form a helix (Craig et al. 1971). The rate of helix dissociation depends on the number of base pairs that must break to form the intermediate and this is a function of chain length and the on-rate and stability constant for each pair. Under force, F, the stability constant, s_f, will fall exponentially as:

$$s_f = s\exp\left(-\left(Fx_b + Fx_f\right)/k_BT\right) \quad (5)$$

where x_f and x_b are the widths of the barriers to association and dissociation, respectively, for each base pair interaction. If the forward barrier is assumed to be small in width compared to the dissociation length, x_b, and the on-rate suppressed under force, then we can obtain an on-rate for our 12 base pair ($N = 12$) oligonucleotide since:

$$\begin{aligned} v &\approx 2Nk_f\exp\left(-\left(N\Delta G_{bp} - FNx_b\right)/k_BT\right) \\ &= 2Nk_f\exp\left(-\left(\Delta G' - Fx_\beta\right)/k_BT\right) \end{aligned} \quad (6)$$

where $\Delta G'$ is the energy change on rupture, taken here to equal E_r from the force spectroscopy data as being between 9 and 13 kcal mol^{-1}.

We calculate an on-rate, k_f, per base pair of 4×10^5 to 4×10^7 s^{-1}, which has been estimated previously as between 10^6 and 10^7 s^{-1} from experimental relaxation times (Craig et al. 1971). Although capable of deriving on rate values of reasonable agreement, this model assumes that the association and dissociation kinetics of GC and AT base pairs are identical. The model exhibits this limitation with short oligonucleotides, in particular those with AT or GC tracts such as ours (Anshelevich et al. 1984).

Discussion

Presented here is an experimentally determined energy landscape traversed as a dodecamer oligonucleotide is dissociated to its single-stranded counterparts. Furthermore, the general form of this landscape is supported by recent molecular modelling predictions by MacKerrel and Lee (1999) in which they describe an essentially barrierless transition to stretch, followed by a sharp barrier to melt situated at a distance of 2.37 times the contour length of B-DNA. Through force spectroscopy, we have shown that a short 12-mer oligonucleotide is ruptured under loading rates below 3000 pN s^{-1} with a statistical force no greater than 40 pN. The duplex is also known to undergo a structural change (here attributed to a stretch) under the loads employed with a force less than 17 pN. However, for long DNA, the over-stretched S-DNA form is found reproducibly at forces near 70 pN, which is independent of both length and the experimental loading rates accessible to AFM (Rief et al. 1999). The characteristic plateau observed in these force distance curves, indicating the highly cooperative B $\rightarrow$ S transition, is not identifiable in the force extension curves of our 12-mer, and indeed would not be for a system out of equilibrium and held under a weak force. Since stretching of our oligonucleotide occurs here at forces that are significantly lower than 70 pN, without any evidence of a B $\rightarrow$ S force plateau, it can be inferred that stretching of short DNA involves a non-cooperative process. Therefore, it is expected that the cooperativity of the B $\rightarrow$ S transition increases with length.

Recently, Strunz et al. (1999) have published dynamic force spectroscopy data of DNA melting for 10, 20 and 30 base pairs in length. Importantly, this has enabled us to compare our 12-mer data to a similar study. Both studies have used dynamic force spectroscopy to reveal the inter-relationship between unbinding force and rate of loading for short DNA rupture. In comparison to earlier studies, in which high rupture forces were measured for single experimental loading rates, these two dynamic force spectroscopy studies are in very close agreement. Both studies reveal much lower forces, 22 to 53 pN over loading rates ranging from 16 to 4000 pN s^{-1} for 10, 20 and 30-mer DNA (Strunz et al. 1999), and 17 to 40 pN over loading rates ranging from 100 to 3000 pN s^{-1} for our 12-mer DNA. Also in reasonable agreement is that the energy barrier to rupture is situated only a few angstroms from an energy minimum. The thermal off-rate measured for 10-mer DNA (Eq. 2) suggests a barrier of height to rupture of less than 16 kcal mol^{-1} (Strunz et al. 1999). Additionally, Strunz's data revealed that this energy landscape distance is proportional to the number of base pairs. An important question arises when we consider whether or not this single energy barrier probed by AFM is the only barrier present in the force-induced melting landscape. Thermal melting studies have allowed prediction of the energy required for both the stretch and rupture processes. As discussed earlier, the shape of the energy landscape in the stretch region corresponds to a much lower thermal force scale of approximately 1 pN; hence, probing this region of the energy landscape would require rates of loading many orders of magnitude lower than those accessible to AFM, using a technique such as the biomembrane force probe (Evans et al. 1995).

Whilst our data suggest that a transition occurs under forces lower than 17 pN for 12-mer DNA, contradictory data have been presented by Noy et al. (1997) where, for a 14-mer oligonucleotide, plateaus in the force extension curves at 120 ± 50 pN were evident. Furthermore, these former studies revealed rupture forces of several hundred piconewtons [460 pN of Noy et al. (1997), 410 pN of Lee et al. (1994), which are equivalent to over 60 kcal mol^{-1} nm^{-1}]. MacKerell and Lee (1999) show a distribution of rupture forces for a repetitive sequence DNA with five possible binding orientations with its complementary partner. The distribution, drawn from 45 measurements, has indications of three peaks at 130, 330 and 490 pN, attributed by the authors to rupture of 12, 16 and 20 base pairs. However, more measurements are required to verify this conclusion since the distribution is

broad. Force distributions drawn from a significantly larger sampling number (200–400) and only one possible binding orientation were published by Strunz et al. (1999). Oligonucleotides of 10, 20 and 30 base pairs showed probable rupture forces between 22 and 53 pN. Clearly the unbinding pathway may differ between thermal and force-induced melting and here we have used thermal studies to place a lower bound on the energy involved in rupture. The free energy change on rupture for the duplex used by Noy et al. (1997) is approximately 13 kcal mol^{-1} (Breslauer et al. 1986) and the 460 pN rupture force was attributed to a 307.7 kcal mol^{-1} change in enthalpy plus work done in stretching the duplex. Molecular simulation, where the pathway is constrained by high rates of duplex separation, does not help greatly in the interpretation of this change in energy. Simulations by MacKerell and Lee (1999), for instance, show a free energy change on rupture of 4.7 kcal mol^{-1} for a 12-mer, compared to the 12.4 kcal mol^{-1} predicted (Breslauer et al. 1986) for the sequence. This study did suggest that the adiabatic limit for force (the maximum energy gradient) is around 130 pN, which too contradicts the earlier AFM studies. In fact, this value of rupture force is close to that measured for long strands of DNA. Adiabatic mapping of the dissociation of short oligonucleotides reveals a landscape, but the neglect of thermal motion distorts the energies considerably. In addition, such computations are affected by the choice of force field and nature of the constraints imposed. The adiabatic limit from studies by Lebrun and Lavery (1998) of a 14-mer is 540 pN. It is reasonable to expect that short oligonucleotides have considerable, if not uninhibited, thermal motion during the force rupture experiment since the duplex is formed under identical conditions of force as the tip is approached to the surface. Where thermal motion is restricted, a duplex would not form on tip approach. Indeed, this is seen in the AFM measurements of long DNA strands (Rief et al. 1999).

It is predicted that a short oligonucleotide can undergo several types of transition from the double helix to single strands, including untwisting, stretching, strand separation and combinations of these (Olson and Zhurkin 2000). The constraints and forces required to entice a particular melting pathway are undoubtedly different and will exist in different experimental and computational strategies. For example, the force loading rates in simulation would bias the transition to one of stretch, whereas we believe experimental force measurements, in which the molecule is sampling a considerable part of configurational space, would permit strand separation, through alternative structural transitions. Whilst the mechanical nature of the helix changes with these transitions, such as stiffening, direct measurements of these properties for short oligonucleotides are not possible from this force experiment. The assumption of a transition from the force data presented here is evident from the missing energy that is needed for strand separation. However, measurements of the mechanical properties can be made using long segments of DNA (Smith et al. 1992, 1996; Léger et al. 1999).

The data published on the rupture forces for short oligonucleotides fall into three groups of force: 20–50 pN (this study and Strunz et al. 1999), 150 pN (MacKerrel and Lee 1999) and 410–460 pN (Lee et al. 1994; Noy et al. 1997). The similarity between this study and that of Strunz suggests that we are investigating the same interaction, and the analysis through force spectroscopy indicates that this interaction is probed in a thermally active regime. A significant difference between these two studies and those of MacKerell, Lee and Noy are the contact forces that are applied between tip and surface on approach. To minimize non-specific interactions and distortion of the tip and sample surfaces, the contact force in this study is kept below 200 pN, and in the study by Strunz, lower than 150 pN. However, the data presented in the other studies suggest that the contact force often exceeds 1 nN. The necessity for low contact forces to measure single-molecular interactions successfully is well documented (Evans et al. 1991, 1995; Merkel et al. 1999), and may explain the large differences in reported rupture forces.

Summary

Despite considerable conformational flexibility it has been shown here that the results of dynamic force spectroscopy of a short oligonucleotide can be interpreted through the theory of Kramers (Kramers 1940; Hanggi et al. 1990). A combination of thermal melting studies and force spectroscopy reveals that the short duplex undergoes a conformational change under forces below 17 pN before rupture. The free energy of base pair dissociation is determined here around 1 kcal mol^{-1} and each base pair has an association rate constant between 4×10^5 and 4×10^7 s^{-1}. Since it is known that the interaction potentials of CG and AT are different (Rief et al. 1999), short oligonucleotides provide a means by which sequence specificity of dissociation energetics can be explored. Such studies, however, will necessitate the refinement of appropriate helix-coil transition and melting models. Furthermore, it is clear that continued single-molecule dynamic force spectroscopy studies, possibly using complementary experimental techniques such as AFM and the biomembrane force probe, are required to extend our knowledge of the energetics of DNA and its sequence-dependent nature. Insights into energy pathways provide a greater understanding of the mechanisms and interactions that underpin the control of biological processes.

Acknowledgements We would like to thank Professor E. Evans (Department of Physics, The University of British Columbia, Vancouver, Canada) for his time spent in many valuable discussions. We are grateful to M. Lomas (School of Pharmaceutical Sciences, The University of Nottingham) for the design and construction of the AFM used for this research. We are very grateful to S. Allen and S. Harris (School of Pharmaceutical Sciences, The

University of Nottingham) for many important discussions. We thank Mr. G. Shepperd for technical support. The undecanol-thiol was a gift from Stephan Vansteenkiste, University of Gent, Gent, Belgium. L.H.P. acknowledges funding from the BBSRC. The development of the force microscope was funded through the EPSRC Analytical Chemistry Programme. Collection of the XPS data was undertaken courtesy of VG Scientific, East Grinstead, UK, with thanks in particular to Kevin Robinson, Matthew Fitzpatrick, Richard White and Alison Moyes.

References

Anshelevich VV, Vologodskii AV, Lukashin AV, Frank-Kamenetskii MD (1984) Slow relaxational processes in the melting of linear biopolymers: a theory and its application to nucleic acids. Biopolymers 23: 39–58

Balsera M, Stepaniants S, Izrailev S, Oono Y, Schulten K (1997) Reconstructing potential energy functions from simulated force-induced unbinding processes. Biophys J 73: 1281–1287

Bell GI (1978) Models for the specific adhesion of cells to cells. Science 200: 618–627

Breslauer KJ, Frank R, Blöcker H, Marky LA (1986) Predicting DNA duplex stability from the base sequence. Proc Natl Acad Sci USA 83: 3746–3750

Cleveland JP, Manne S, Bocek D, Hansma PK (1993) A non-destructive method for determining the spring constant of cantilevers for scanning force microscopy. Rev Sci Instrum 64: 403–405

Cluzel P, Lebrun A, Heller C, Lavery R, Vivoy J-L, Chatenay D, Caron F (1996) DNA: an extensible molecule. Science 271: 792–794

Craig ME, Crothers DM, Doty P (1971) Relaxation kinetics of dimer formation by self complementary oligonucleotides. J Mol Biol 62: 383–401

Evans E (1999) Energy landscapes of biomolecular adhesion and receptor anchoring at interfaces explored with dynamic force spectroscopy. Faraday Discuss 111: 1–16

Evans E, Ritchie K (1997) Dynamic strength of molecular adhesion bonds. Biophys J 72: 1541–1555

Evans E, Ritchie K (1999) Strength of a weak bond connecting flexible polymer chains. Biophys J 76: 2439–2447

Evans E, Berk D, Leung A (1991) Detachment of agglutinin-bonded red blood cells. Biophys J 59: 838–848

Evans E, Ritchie K, Merkel R (1995) Sensitive force technique to probe molecular adhesion and structural linkages at biological interfaces. Biophys J 68: 2580–2587

Grubmüller H, Heymann B, Tavan P (1996) Ligand binding: molecular mechanics calculation of the streptavidin biotin rupture force. Science 271: 997–999

Hanggi P, Talkner P, Borkovec M (1990) Reaction rate theory – 50 years after Kramers. Rev Mod Phys 62: 251–342

Hegner M, Wagner P, Semenza G (1993) Ultralarge atomically flat template-stripped Au surfaces for scanning probe microscopy. Surf Sci 291: 39–46

Konrad MW, Bolonick JI (1996) Molecular dynamics simulation of DNA stretching is consistent with the tension observed for extension and strand separation and predicts a novel ladder structure. J Am Chem Soc 118: 10989–10994

Kramers HA (1940) Brownian motion in a field of force and the diffusion model of chemical reactions. Physica (Utrecht) 7: 284–304

Lebrun A, Lavery R (1998) Modelling the mechanics of a DNA oligomer. J Biomol Struct Dyn 16: 593–604

Lee GU, Chrisey LA, Colton R (1994) Direct measurement of the forces between complementary strands of DNA. Science 266: 771–773

Léger JF, Romano G, Sarkar A, Robert J, Bourdieu L, Chatenay D, Marko JF (1999) Structural transitions of a twisted and stretched DNA molecule. Phys Rev Lett 83: 1066–1069

MacKerrel AD, Lee GU (1999) Structure, force, and energy of a double-stranded DNA oligonucleotide under tensile loads. Eur Biophys J 28: 415–426

Merkel R, Nassoy P, Leung A, Ritchie K, Evans E (1999) Energy landscapes of receptor-ligand bonds explored with dynamic force spectroscopy. Nature 397: 50–53

Nakano S, Fujimoto M, Hara H, Sugimoto N (1999) Nucleic acid duplex stability: influence of base composition on cation effects. Nucleic Acids Res 27: 2957–2965

Noy A, Vezenov DV, Kayyem JF, Meade TJ, Lieber CM (1997) Stretching and breaking duplex DNA by chemical force microscopy. Chem Biol 4: 519–527

Olson WK, Zhurkin VB (2000) Modeling DNA deformations. Curr Opin Struct Biol 10: 286–297

Park PJ, Sung W (1999) Dynamics of a polymer surmounting a potential barrier: the Kramers problem for polymers. J Chem Phys 111: 5259–5266

Petersheim M, Turner DH (1983) Base-stacking and base-pairing contributions to helix stability: thermodynamics of double-helix formation with CCGG, CCGGp, ccGGAp, ACCGGp, CCGGUp and ACCGGUp. Biochemistry 22: 256–263

Pörschke D (1977) Elementary steps of base recognition and helix-coil transitions in nucleic acids. Mol Biol Biochem Biophys 24: 191–218

Press WH, Teukolsky SA, Vetterling WT, Flannery BP (1992) Numerical Recipes in C. Cambridge University Press, Cambridge, pp 408–412

Rief M, Clausen-Schaumann H, Gaub H (1999) Sequence-dependent mechanics of single DNA molecules. Nat Struct Biol 6: 346–349

Simson DA, Strigl M, Hohenadl M, Merkel R (1999) Statistical breakage of single protein A-IgG bonds reveals crossover from spontaneous to force-induced bond dissociation. Phys Rev Lett 83: 652–655

Smith SB, Finzi L, Bustamante C (1992) Direct mechanical measurements of the elasticity of single DNA molecules by using magnetic beads. Science 258: 1122–1126

Smith SB, Cui Y, Bustamante C (1996) Overstretching B-DNA: the elastic response of individual double-stranded and single-stranded DNA molecules. Science 271: 795–799

Strunz T, Oroszlan K, Schäfer R, Guntherödt H (1999) Dynamic force spectroscopy of single DNA molecules. Proc Natl Acad Sci USA 96: 11277–11282

Sugimoto N, Nakano S, Yoneyama H, Honda K (1996) Improved thermodynamic parameters and helix initiation factor to predict stability of DNA duplexes. Nucleic Acids Res 24: 4501–4505

Willemsen OH, Snel MME, Kuipers L, Figdor CG, Greve J, De Grooth BG (1999) A physical approach to reduce nonspecific adhesion in molecular recognition atomic force microscopy. Biophys J 76: 716–724

Williams PM, Moore A, Stevens MM, Allen S, Davies MC, Roberts CJ, Tendler SJB (2000) On the dynamic behaviour of the forced dissociation of ligand-receptor pairs. J Chem Soc Perkin Trans 2 5–8